REVIEW

Toward visualization of nanomachines in their native cellular environment

Jason Pierson · Musa Sani · Cveta Tomova · Susan Godsave · Peter J. Peters

Abstract The cellular *nanocosm* is made up of numerous types of macromolecular complexes or biological nanomachines. These form functional modules that are organized into complex subcellular networks. Information on the ultra-structure of these nanomachines has mainly been obtained by analyzing isolated structures, using imaging techniques such as X-ray crystallography, NMR, or single particle electron microscopy (EM). Yet there is a strong need to image biological complexes in a native state and within a cellular environment, in order to gain a better understanding of their functions. Emerging methods in EM are now making this goal reachable. Cryo-electron tomography bypasses the need for conventional fixatives, dehydration and stains, so that a close-to-native environment is retained. As this technique is approaching macromolecular resolution, it is possible to create maps of individual macromolecular complexes. X-ray and NMR data can be 'docked' or fitted into the lower resolution particle density maps to create a macromolecular atlas of the cell under normal and pathological conditions. The majority of cells, however, are too thick to be imaged in an intact state and therefore methods such as 'high pressure freezing' with 'freeze-substitution followed by room temperature plastic sectioning' or 'cryo-sectioning of unperturbed vitreous fully hydrated samples' have been introduced for electron tomography. Here, we review methodological considerations for visualizing nanomachines in a close-to-physiological, cellular context. EM is in a renaissance, and further innovations and training in this field should be fully supported.

Introduction

Proteins perform key roles in the majority of cellular functions. They also serve as building blocks for larger heterogeneous macromolecular assemblies, or biological nanomachines, which are organized into cellular 'modules' (Alberts 1998). As the name implies, a biological machine is analogous to the man-made version. Both are made of individual components that function in a coordinated fashion to perform specific functions. In nature, if any single structural component of a nanomachine malfunctions the result is often a disease. Discerning the ultra-structure of a biological machine and its components within the cell can contribute to an understanding of how it functions both normally, and in disease. Little is known, however, about the details of how these macromolecular machines are spatially organized within a cellular environment.

X-ray crystallography and NMR approaches have been used to complement genetics, biochemistry, and proteomics to characterize the overall structural organization of individual protein complexes. Most macromolecules, however, cannot be crystallized, or when crystallized, they diffract poorly, as only large, well-ordered crystals diffract. In the

J. Pierson · M. Sani · C. Tomova · S. Godsave · P. J. Peters (✉)
Division of Cell Biology,
The Netherlands Cancer Institute - Antoni
van Leeuwenhoek Hospital (NKI-AVL),
Plesmanlaan 121 B6, 1066 CX Amsterdam, The Netherlands
e-mail: p.peters@nki.nl
URL: www.nki.nl/research/peters

case of NMR, the size of the protein complex is limited to approximately < 100 kDa (Wider and Wüthrich 1999). In order to study biological machines where they normally reside, and not as isolated entities, then more suitable imaging techniques, such as electron microscopy (EM) and electron tomography (ET), need to be adapted.

Transmission EM is one of the most powerful techniques for ultra-structural studies of the cell and its constituents (McIntosh 2001). When performed on sections of fixed cells and tissues, it has been invaluable in establishing a picture of the subcellular arrangement of organelles and determining the localization of gene products with immunogold labeling techniques. As an example, recently, the route of tubercle bacillus infection was demonstrated using immunogold labeling on aldehyde fixed cryo-sections and our findings revealed a pathway that is against the current textbook dogma (van der Wel et al. 2007). Nevertheless, this technique makes use of fixed, dehydrated and heavy metal-stained material, and artifacts at the macromolecular level may be introduced at all stages (Peters and Pierson 2008). Recently, there has been an important focus on optimal sample preservation for high-resolution structural studies of macromolecules in situ. This quest to find the true relation between molecules, linked into supramolecular complexes and assembled into an intricate network of cellular compartments, is revolutionizing modern transmission EM. The catalyst for this revolution has been cryo-ET (Dubochet et al. 1988; Lucic et al. 2008). ET is used to generate 3D maps from a series of 2D transmission EM images. The specimen is rotated with respect to the imaging source; in this case, electrons and a series of projection images are recorded over a limited angular range (usually −70° to +70°).

Cryo-ET is based on a freezing technique that captures the cellular water in an amorphous (glass-like) layer in which all cellular components are embedded. This process is known as vitrification, which is achieved by the ultra-rapid freezing of a thin biological sample, circumventing all harsh chemical fixatives and heavy metal stain.

Here we analyze different EM imaging procedures that have the ultimate goal of visualizing macromolecular 'machines' in the most natural environment currently possible. Using a variety of imaging techniques, structural information can be extracted at different resolution levels. This information can be combined to create a multi-resolution density map of the individual macromolecular complexes; eventually leading to a catalog of all biological nanomachines that can be used to search in 3D volumes (Bohm et al. 2000) of cells, and to determine the spatial organization of individual complexes within a cellular environment (Nickell et al. 2006). In addition, we give insight on what will be important for the future to achieve this goal of mapping macromolecular machines within a cellular context.

Single particle analysis

Electron microscopy has provided important structural information about protein complexes essential for describing their functional organization. Single particle analysis (SPA) has been used to determine the structure of a variety of macromolecules and biological nanomachines. This involves the analysis of images from large numbers of purified, macromolecular particles that have been placed on an EM grid. These images are used to build up a 3D model of the complex.

Sample preparation

For SPA, a convenient isolation approach is to 'fish' the nanomachines out from their cellular environment using a tag that targets a single component of the complex, most importantly often in a single step (Kelly et al. 2008). Negative staining is often the first step to check for quality and suitability. The sample is embedded in heavy metal salts, such as uranyl acetate or phosphotungstic acid, providing a contrasting agent for the weakly electron-scattering biological molecules. This staining has been part of the most commonly used EM preparation methods since its introduction 50 years ago (Brenner and Horne 1959). An example can be seen in Fig. 1 that shows a negatively stained *S. flexneri* needle appendage. The averaged projection view shows the basal part of the needle complex, composed of several rings that traverse the cell envelope. The heavy metal stain can, however, create a cast around the surface of the specimen. Moreover, dehydration of the specimen can potentially alter fine structural details. It also imposes a resolution limit of 10–20 Å (Amos et al. 1982; Sani et al. 2007). These limitations have been overcome by cryo-fixation, or embedding of the specimen in vitreous water (Dubochet et al. 1988).

Image analysis

Irrespective of the sample preparation method, individual particles must be aligned and averaged to improve the signal. For cryo-preparation methods the averaged particle can contain information to atomic resolutions (Henderson 1995; van Heel et al. 2000), but suffer from limited contrast. The imaging electron dose is limited (low-dose imaging) to 10–20 electrons/Å^2 (Glaeser and Taylor 1978; Dubochet et al. 1988) to reduce the number of inelastically scattered electrons (Stark et al. 1996) that often lead to radiation damage. To overcome this problem, single particle image enhancement programs have been developed (van Heel et al. 1996; Frank et al. 1996) to average large numbers of copies of single particles and improve the signal-to-noise ratio.

The first step in the averaging procedure is to identify individual particles within the micrograph manually or
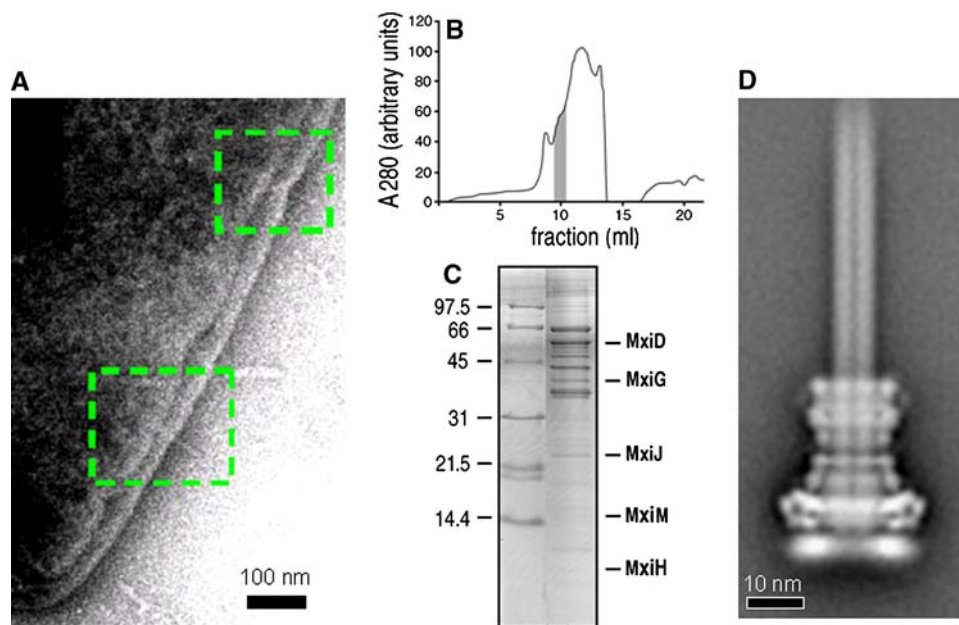
Fig. 1 From a whole cell to isolated complexes. **a** Electron micrographs of osmotically shocked *S. flexneri* exhibiting the type III secretion system protruding through the bacterial envelope (see *boxed area*). **b** Gel chromatography of solubilized secretion complexes from the bacterial envelope. **c** The fraction containing enriched complex is checked by SDS and individual bands identified by mass spectrometry. **d** 2D projection average of 1,500 isolated needle complexes composed of a hollow needle appendage (indicated by a stain-penetrated line along its axis) and a basal part of several rings that traverse the cell envelope. The channel that runs through the needle appendage is 2–3 nm in diameter indicating that substrates that exit the conduit do so in an unfolded state

by using semi-automated computer programs. Particle alignment then modifies the rotational and translational position of each particle, such that all particles have a comparable orientation and key features will become visible. Since the resolution depends on the accuracy of the particle alignment, there must be sufficient particle feature recognition in a noisy image. Larger complexes are easier to align and subsequently process. A minimum particle size of 1,000 kDa is therefore desired for proper alignment (Henderson 1995). The more particles used in the reconstruction, the higher the resolution of the final model. The technique is most powerful when the particles display intrinsic icosahedral (Böttcher et al. 1997), helical (Miyazawa et al. 2003), or crystalline (Henderson et al. 1990) symmetry, that in certain instances such as polyhedrosis virus (Yu et al. 2008), aquaporin-1 (Murata et al. 2000; Engel 2003) and of the bacterial flagellum (Yonekura et al. 2003) have reached atomic resolution.

Asymmetric complexes continue to remain challenging to images using SPA. The ribosome, which is one of the most analyzed low symmetry single particles, is an exception. It has served for many years as test specimen in the development of many single particle techniques (Stark 2002). Although the resolution is lower for such asymmetric particles, a quantitative description, on the quaternary level, is nevertheless possible.

Visualizing nanomachines in a cellular context

A drawback with the single particle technique is that the nanomachines may undergo changes during isolation, such as loss of labile components, or certain conformational states may be favored. Furthermore, there are many macromolecular assemblies associated with membranes, which should be studied without extraction, in a cellular context.

Specimen preservation is one of the most critical steps in the entire process of native cellular imaging. Cellular water in liquid form is incompatible with the vacuum of the EM. Water is the most abundant cellular constituent and therefore important for preserving cellular ultra-structure. Currently the only way to fix cellular constituents without introducing significant structural alterations is by cryofixation. To be successful, the freezing process has to be ultra-rapid in order to avoid ice crystal formation, which damages cellular material and can hinder imaging. There are currently two common methods employed; plunge freezing into liquid ethane (Dubochet et al. 1988) and high pressure freezing (HPF, Studer et al. 2001).

Cryo-fixation

The plunge freezing technique is suitable for samples with limited thickness [i.e., bacteria, isolated cellular organelles

(Nicastro et al. 2006) or viruses] or relatively thin regions of larger cells (Medalia et al. 2002). The physical properties of water, namely its poor heat conductivity, are the reason that freezing is limited for large cells and tissues. Currently, the only method to vitrify thicker samples (up to 200 μm) is by HPF.

The high pressure introduced at the moment of freezing lowers the freezing point of water. Synchronized pressurization and cooling of the sample takes place within 20 ms (Studer et al. 2008). The development of this technique has allowed samples of various thicknesses to be vitrified, although vitrification of most mammalian cells in the absence of non-isotonic cryo-protectants has not yet been established. Cryo-fixation has two distinct advantages over chemical fixation. It is achieved within milliseconds and it ensures simultaneous immobilization of all macromolecular components. Many protein networks are very labile and fall apart with the slightest osmotic or temperature change and these unwanted effects are minimized during cryo-fixation. These techniques allow the study of biological samples with improved ultra-structural preservation, and can facilitate the study of dynamic processes.

Freeze-substitution

Achieving optimal preservation of the biological sample is undoubtedly critical, but still only the first step in visualizing it. Until it was demonstrated that vitreous water could be sectioned and cellular structure visualized directly in the cryo-EM (Dubochet et al. 1988), the only way of examining the cryo-fixed sample was by embedding it in resin for sectioning. For this the vitrified water in the HPF frozen specimen must be replaced by an organic solvent in a process known as freeze-substitution (FS).

Freeze-substitution is a process of dehydration, performed at temperatures low enough to avoid the formation of ice crystals and to circumvent the damaging effects observed after ambient-temperature dehydration. Aggregation of macromolecules in organic solvents and changes of the hydration shell surrounding the biological molecules can occur even at very low temperatures, but it is reasonable to assume that FS at temperatures below a specific threshold preserves the hydration shell (Hobot et al. 1985; Kellenberger 1991). Further, the total or partial loss of the hydration shell can be reduced during the cryo-embedding procedure, so minimizing aggregation and the redistribution of diffusible elements (Edelman 1991; Quintana et al. 1991).

Freeze-substitution combines instant physical immobilization of the cell constituents and resin embedding. Once substitution is complete, samples are gradually warmed-up and processed further as for conventionally prepared samples. Successful cryo-fixation followed by FS shows superior preservation of fine structure compared to chemical fixation techniques (Müller 1992; Steinbrecht and Müller 1987). This technique also gives the possibility of examining thick (200–300 nm sections) samples by ET, so that relatively large cellular volumes can be studied in 3D. This approach is very beneficial for an understanding of the complex relation between different cellular organelles and randomly occurring events. Membrane contact sites between the ER and the outer-most membrane of the apicoplast (a plastid found in most parasites from Apicomplexa *Toxoplasma gondii* and *Plasmodium* species) can be seen in Fig. 2 as an example of a sample that has been freeze-substituted in 0.1% uranyl and embedded in Lowicryl HM20 (Tomova et al. 2009). In addition, this image shows the potential that HPF/FS has in combining optimal structural preservation with protein detection and for applying ET to thick sections. There are numerous examples where HPF/FS combined with ET have changed our understanding of cellular structure and dynamics (Marsh et al. 2001; Murk et al. 2003; Perkins et al. 2001; Perktold et al. 2007; Tomova et al. 2006; Zeuschner et al. 2005). Recently, it was shown that cellular fibrils connect protofilaments directly to the inner kinetochore (McIntosh et al. 2008), which nicely illustrates a mechanism for directly harnessing microtubule dynamics for chromosome movement.

Even though numerous different substitution protocols exist, there are only a few methodological investigations concerning the process of FS, such as the replacement of ice by an organic solvent at temperatures of −90 to 0°C (Müller et al. 1980), the substitution capacities of different organic solvents in the presence of water (Humbel and Müller 1986), and the influence of the different solvents on the ultra-structural preservation of high-pressure frozen, freeze-substituted samples (Studer et al. 1995). It is still arguable what alterations of the cellular structure are induced and to what extent the information obtained can be considered as an accurate representation of the living cell, especially in the case of the 3D structure of macromolecules.

Vitreous cryo-sectioning

The expansion and development of cryo-ET and cryo-sectioning of native vitreous samples such as yeast and bacteria has made it possible to visualize cells directly in the absence of chemicals, heavy metals and hypertonic cryo-protectants. Vitreous cryo-sections of *Saccharomyces cerevisiae* (Fig. 3) showed that the nuclear envelope forms a unique membrane contact site with the vacuole, called the nucleus–vacuole (NV) junction (Millen et al. 2008). 'Velcro'-like protein–protein interactions hold the junction in place. The proteins involved are Vac8 in the vacuole
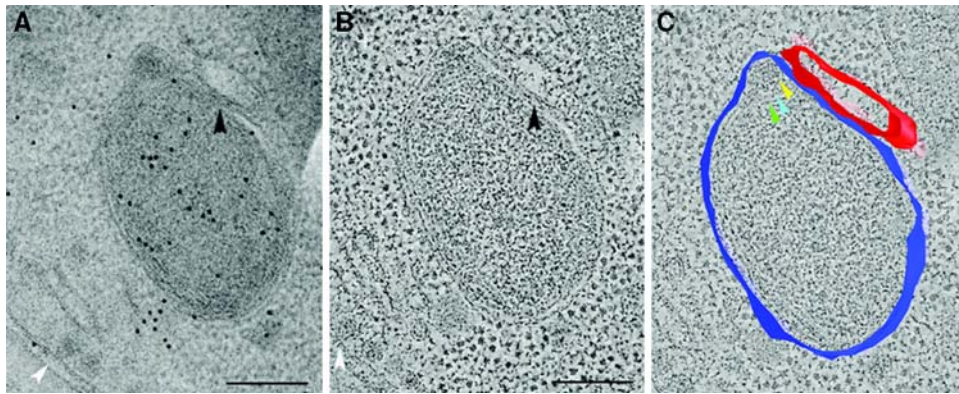
Fig. 2 High pressure freezing/FS combined with ET reveals the relation between cellular compartments. Images illustrating the relation between the ER and the apicoplast (a plastid acquired by secondary endosymbiosis) outermost membrane in the parasite *Toxoplasma gondii*. **a** Image from the aligned tilt stack acquired from a thick section (200 nm), at −35° tilt. The gold particles, used for also for the alignment of the series, are specific labeling for the apicoplast specific Acyl carrier protein. The relation between the membranes of the ER and the apicoplast is pointed (*black arrowhead*). **b** Optical slice from the tomo-graphic reconstruction of the same apicoplast. The lamellar structure of all the membranes is visible. No additional contrasting was applied. The close alignment of the outermost apicoplast membrane and the ER is pointed (*black arrowhead*). **c** View of a model generated by the tomographic reconstructions sown in **b**. Additional observation in these images is the budding of vesicles from the nuclear envelope (*white arrowhead*). Sample substituted in 0.1% uranyl and embedded in Lowicryl HM20. Sections were not post-stained. The scale bars in **a** and **b** are 100 nm
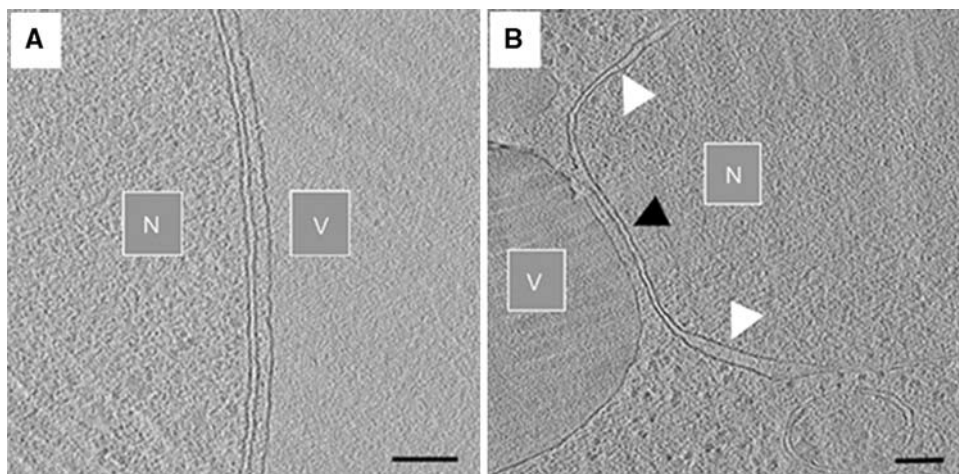

Fig. 3 Tomography of thin vitreous cryo-sections of the *Saccharomyces cerevisiae* nucleus–vacuole junction. **a** A 10-nm slice from a reconstruction that shows the consistent width of the nuclear membranes in relation to the vacuole. '*N*' denotes the nucleus and '*V*' the vacuole. Scale bars 50 nm. **b** A second reconstruction that shows more of an overview of the region of the NV junction. The inner and outer membranes of the bulk nuclear envelope (*white arrows*) are further apart compared to those of the nuclear envelope at the NV junction. *Around and within* the nucleus, macromolecular complexes can be observed, along with a mitochondrion at the *bottom* of the image

membrane, which is associated with Nvj1 in the outer nuclear membrane. NV junctions are the site of piecemeal microautophagy of the nucleus, which is a type of autophagy that targets portions of the nucleus.

Artifacts induced by the process of sectioning (knife marks, crevasses, and compression) have been described in detail and must be taken into consideration (Al-Amoudi et al. 2005). An example of a crevasse is shown in Fig. 3b, where crevasses are partially visible in the vacuole (V) as white stripes perpendicular to the cutting direction (parallel to the NV junction). In certain cases crevasses can penetrate into the depths of the cryo-section of a vitreous sample and affect the underlying biological ultra-structure, however, in ultra-thin sections (< 50 nm) these artifacts appear to be non-intrusive to the biological ultra-structure.

It is possible to minimize knife marks and crevasses, making compression the most problematic artifact. Compression is a deformation that makes the vitreous section shorter along the cutting direction without changing the overall volume. The result is an increase in overall section thickness. Thirty percent compression within vitreous cryo-sections is not unusual. If compression is evenly distributed, then a reverse transform (Al-Amoudi et al. 2005) can be applied to the entire volume post-reconstruction. However we
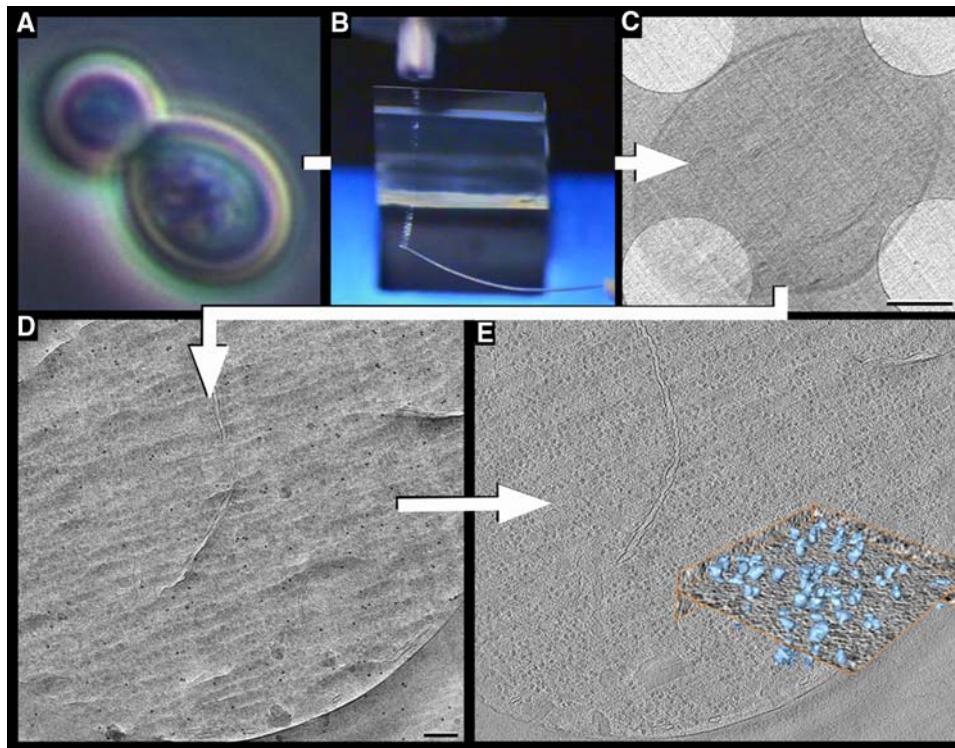
Fig. 4 A diagram illustrating the vitreous cryo-sectioning technique. **a** A confocal laser image of *Saccharomyces cerevisiae* (Dr Maxim Zakhartsev and Doris Petroi, International University Bremen, Germany). The cells are rapidly frozen by high pressure freezing (HPF) in copper tubes and then sliced (**b**) into very thin (50 nm) vitreous cryosections. **b** A relatively long ribbon of vitreous cryosections is held by the operator and pulled away from the diamond knife. The ribbon is placed on an EM grid and imaged by Cryo-EM and -ET. **c** A medium magnification single image showing a 50 nm vitreous slice of a single *Saccharomyces cerevisiae* cell. Scale bar 2 µm. In the corner of the image are *holes* within the carbon support film (*white round circles*).

Subsequent cryo-ET is shown in **d, e**. **d** A single 2D projection image from a tilt series. It is difficult to interpret such images due to the projection problem of overlapping structures, along with a low signal-to-noise ratio and contrast levels. Scale bar 100 nm. **e** Multiple single projection images can be aligned and reconstructed into a 3D volume (in this case using IMOD (Kremer et al. 1996)). A 5-nm slice from a reconstructed volume. In this image the cellular environment can be visualized much better than in the single projection image (**d**). The inset displays a selected area (*orange-bounded box*) from the tomographic reconstruction (**e**)

have seen indications that compression is rather non-homogeneous in filament bundles (Salje et al. 2009), microtubules (Bouchet-Marquis et al. 2007), desmosomes (Al-Amoudi et al. 2007), and bacterial chemotaxis receptors (Zhang et al. 2004). On the nanomachine level the affect of these artifacts is uncertain, but could be minimal for rigid, macromolecular machinery (J. Pierson et al., unpublished).

In addition, extreme caution must be taken during image acquisition. Beam induced alterations in the sample are well-known to be a problem, and are often believed to be the rate limiting step for achieving optimal cryo-EM. It is no secret that vitreous sections 'flow' during image acquisition (Sartori Blanc et al. 1998; Sartori, et al. 1996), which is considered by some researchers to be due to local charge accumulation and/or radiochemical processes. Therefore, it is important to 'learn' how to read vitreous sections with respect to structural integrity and preservation (Dubochet et al. 2007). A common practice is to acquire a single projection image, using a very low electron dose, before a tilt series is collected, and then compare it to an image taken

after the series is complete. If there is no noticeable change, then the structural integrity of the vitreous section has been maintained. If the final image appears 'smooth' (with no knife marks and/or crevasses visible) then the ultra-structure of the cell must be analyzed with caution. Map montaging helps to reduce the 'overhead' electrons used to pinpoint an area of interest before acquiring a tilt series. In order to preserve the vitreous section integrity, the electron beam dose is restricted, which in turn limits the contrast levels and the signal-to-noise ratio. This makes subsequent analysis of such images rather difficult.

The application of tomography of vitreous sections is the future of cellular imaging, combining close-to-native preparation techniques with a 3D view of the vitreous section. The ultimate goal is to map complex macromolecular machines within 3D slices of large cells and tissue. An example is shown of a sample of *Saccharomyces cerevisiae* that was immobilized in a copper tube using HPF. The sample was vitreous cryo-sectioned into thin (50 nm) slices and observed using cryo-ET (Fig. 4).
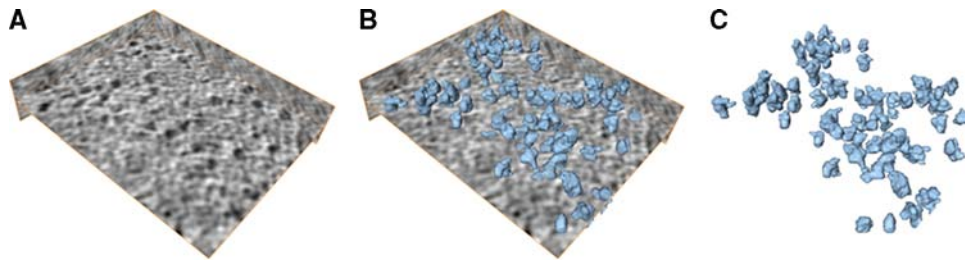
Fig. 5 Charting macromolecular machines within a vitreous cryo-section. **a** A selected area (*orange-bounded box* in Fig. 4d) from a tomographic reconstruction. **b, c** The volume has been surface rendered in order to visualize the cellular organization of macromolecular complexes within a thin vitreous cryo-section from a whole *Saccharomyces cerevisiae* cell

Within the volume of the reconstruction, individual macromolecular complexes can be observed (Fig. 5). Based on their size and distribution we assume that these are native 80S ribosomes in various conformational states, which can also be associated with a variety of protein complexes that aid in protein translation. The true identity, however, remains subjective until a suitable labeling or correlative approach is developed for the vitreous cryo-sectioning.

The future of charting nanomachinery in a native cellular context

We have witnessed light microscopy breaking the diffraction barrier, and in the future the spatial resolution will only improve, with the development of super-resolution light microscopes. Recently it became clear that the green fluorescent protein (GFP) tag has a 10–50 times better signal-to-noise ratio at cryogenic conditions because of reduced photo-bleaching (Sartori et al. 2007). In combination with EM, correlative cryo-LM–EM offers a promising opportunity to investigate cellular organization (Sartori et al. 2007; Schwartz et al. 2007; Plitzko et al. 2009).

Rather than using a single clonable fluorescent (GFP) tagged construct widely used in light microsocopy, a heavier circular string of five GFP's in tandem could be constructed that would be visible in the rather noisy and low contrast cryo-ET images. In addition, the GFP could be coupled to ferritin or another analog electron dense metallothionein molecule to provide a label for cryo approaches (Mercogliano and DeRosier 2007).

High-resolution structures produced by X-ray crystallography or NMR can be fitted or docked into lower resolution EM images to create a multi-resolution map of the protein structure. Such bridging techniques will be instrumental in providing a more complete understanding of the structure and function of molecular complexes than is possible with a stand-alone technique.

Recently, volumetric averaging, which is based on the single particle averaging techniques presented, was applied to isolated organelles (Nicastro et al. 2006) and to cellular protein complexes involving cadherins in epidermal desmosomes of native skin (Al-Amoudi et al. 2007). In the latter case, a high-resolution X-ray crystal structure was placed into the lower resolution cadherin EM map, which resulted in a multi-resolution map of the cadherin in native epidermal desmosomes.

In our own lab, one aim is to further our knowledge on the mechanism of phagocytosis of *Mycobacterium tuberculosis* in human cells. Contrary to the previously accepted view, we have shown using cryo-immunogold EM that the mycobacteria can translocate from the confines of the phagosomal membranes into the cytosol, where they replicate more rapidly and cause cell death (van der Wel et al. 2007). We are now using SPA to investigate the type VII secretion system in isolated bacteria and ultimately we aim to image mycobacteria in sections of HPF frozen human cells, and to gain an understanding of the mechanism for type VII-mediated translocation. The SPA, X-ray and NMR data can then be docked into the images from vitreous sections to construct a macromolecular map of the tubercle bacillus within the host cell.

'Cutting edge' technology

The only way to look inside large cells and tissue, at a close-to-native preservation, is by HPF and vitreous sectioning for cryo-EM. The diamond knife and accessory tools used for cryo-sectioning are improving, which will tremendously improve both the quality of the vitreous sections and subsequently the quality of the imaging. We foresee that in the near future we will use robotics for section manipulation to make handling even more convenient. An alternative approach to mechanical sectioning is based on focused ion beam milling (Marko et al. 2007). A futuristic 'nano-knife' has also been proposed (Singh et al. 2009) constructed from multi-walled carbon nanotubes. In the future these techniques may be able to reduce the distortions currently caused by mechanical vitreous sectioning with a diamond knife, but at the current state are rather technically demanding and in development.

The future of cryo-electron tomography

The current, rather conservative, approximation of the resolution limit of 4–5 nm is expected to improve as the need for high-resolution structural information steadily increases. The electron source is a suitable starting point for improvement. We have witnessed a dramatic increase in spatial coherence of electrons using a field emission electron gun (FEG) rather than a LaB6 or tungsten filament. As the FEG improves, the induced specimen damage will be further minimized and the resolution may improve.

Contrast is generated differently with unfixed, unstained material. The objective lens is defocused creating phase contrast. By defocusing the objective lens, the contrast transfer function is altered and for high resolution studies it will need to be accurately assessed through the volume of single projection images, which is not trivial compared to single projection images. A comparison between CTF corrected and uncorrected can be seen in chromosome arrangement within mitotic HeLa cell sections (Eltsov et al. 2008).

Electron detectors for image collection are also becoming more sophisticated. The problem of electrons backscattering from the fiberoptic plate into the scintillating layer of a charge couple device in current detectors can be partially solved by direct detection of electrons (a complementary metal-oxide-semiconductor) rather than relying on a scintillating layer (Jin et al. 2008). Remote microscopy control allows users from around the world to operate and control microscopes in a completely different part of world. We have seen that the loading of cryo samples has now become completely automatic thanks to the cryo-autoloader, which is an integral part of the Titan Krios (FEI Company). One million particles taken from several EM grids under cryogenic conditions can be imaged and processed automatically in 1 week (H. Stark, personal communication). This trend should not be limited to imaging but also to the sample preparation.

In the past two decades, scientific challenges in physics, chemistry, and molecular cell biology have moved toward the molecular, nanometer-scale domain. Nanoscience, once only a discipline of theoretical subjects, has now been established as a vibrant multidisciplinary area of research and development.

For EM labs to participate fully in this field, it will be necessary to rationalize EM resources. In the Netherlands for example, about 25 EMs are dispersed throughout the country. Some have old instruments and low scientific impact, while their maintenance (service) costs are high. None have the resources needed to initiate a Dutch EM center as part of the much-needed network of major European centers outlined in the strategic roadmap of the European Strategy Forum for Research Infrastructure (ESFRI). A prerequisite to realizing these potential centers, however, is a source of funds for such a major facility and to merge resources and personal. National cryo-EM centers will be optimally suited to become centers of excellence in specific areas of molecular life science and health and there are scientists in many countries with excellent track records in their respective EM-related fields. With the combined effort, expertise and training as was shown within the EU 3D-EM network, several centers should emerge with brilliant junior and senior principle investigators that should have the right scientific setting for acquiring sufficient research grants to make it self sustainable with the help of bright young scientists. We are working toward generating such a center. For more information please visit http://www.necen.nl.

Summary

The cell is composed of a highly organized network of macromolecular machines addressing the demanding requirements of a living cell. Imaging these 'nanomachines' in a cellular, close-to-native state is not a trivial task. Isolation techniques will continue to be essential in solving the structures of these types of protein complexes by the 'divide and conquer' method (McIntosh 2007). For analysis of these nanomachines in their normal environment, rapidly freezing the cell, and cellular elements, in a vitreous layer of water is currently the only technique that retains a physiological state of the organism or cells before EM imaging. As we have seen (Nicastro et al. 2006), unmatched structural information can be obtained. Using vitreous cryo-sections, Cryo-ET can be extended to any cell and almost all tissue. Yet, one major limitation is the proper vitrification under physiological conditions and the localization of each macromolecular complex, along with their binding partners, throughout the thickness of the vitreous cryo-section. As the field of cellular imaging of nanomachines continues to evolve, we are certain to gain invaluable cell biological insights. We are also likely to see many nanotechnology applications that utilize these elegant cellular machines.

References

Al-Amoudi A, Studer D, Dubochet J (2005) Cutting artifacts and cutting process in vitreous sections for cryo-electron microscopy. J Struct Biol 150:109–121

Al-Amoudi A, Castano-Diez D, Betts MJ, Frangakis AS (2007) The molecular architecture of cadherins in native epidermal desmosomes. Nature 450:832–837

Alberts B (1998) The cell as a collection of protein machines: preparing the next generation of molecular biologists. Cell 92:291–294

Amos LA, Henderson R, Unwin PN (1982) Three-dimensional structure determination by electron microscopy of two-dimensional crystals. Prog Biophys Mol Biol 39:183–231

Bohm J, Frangakis AS, Hegerl R, Nickell S, Typke D, Baumeister W (2000) Toward detecting and identifying macromolecules in a cellular context: template matching applied to electron tomograms. Proc Natl Acad Sci USA 97:14245–14250

Böttcher B, Wynne SA, Crowther RA (1997) Determination of the fold of the core protein of hepatitis B virus by electron cryomicroscopy. Nature 386:88–91

Bouchet-Marquis C, Zuber B, Glynn AM, Eltsov M, Gradenbauer M, Goldie KN, Thomas D, Frangakis AS, Dubochet J, Chretien D (2007) Visualization of cell microtubules in their native state. Biol Cell 99:45–53

Brenner S, Horne RW (1959) A negative staining method for high-resolution electron microscopy of viruses. Biochim Biophys Acta 34:103–110

Dubochet J, Adrian M, Chang JJ, Homo JC, Lepault J, McDowall AW, Schultz P (1988) Cryo-electron microscopy of vitrified specimens. Q Rev Biophys 21:129–228

Dubochet J, Zuber B, Eltsov M, Bouchet-Marquis C, Al-Amoudi A, Livolant F (2007) How to "read" a vitreous section. In: McIntosh JR (ed) Cellular electron microscopy. Academic, New York, pp 385–406

Edelman L (1991) Freeze-substitution and the preservation of diffusible ions. J Microsc 161:217–228

Eltsov M, Maclellan KM, Maeshima K, Frangakis AS, Dubochet J (2008) Analysis of cryo-electron microscopy images does not support the existence of 30-nm chromatin fibers in mitotic chromosomes in situ. Proc Natl Acad Sci USA 105:19732–19737

Engel A (2003) Robert Feulgen Lecture. Microscopic assessment of membrane protein structure and function. Histochem Cell Biol 120:93–102

Frank J, Radermacher M, Penczek P, Zhu J, Li Y, Ladjadj M, Leith A (1996) SPIDER and WEB: processing and visualization of images in 3D electron microscopy and related fields. J Struct Biol 116:190–199

Glaeser RM, Taylor KA (1978) Radiation damage relative to transmission electron microscopy of biological specimens at low temperature. J Microsc 112:127–138

Hegerl R, Hoppe W (1976) Influence of electron noise on three-dimensional image reconstruction. Z Naturforsch 31:1717–1721

Henderson R (1995) The potential and limitations of neutrons, electrons and X-rays for atomic resolution microscopy of unstained biological molecules. Q Rev Biophys 28:171–193

Henderson R, Baldwin JM, Ceska TA, Zemlin F, Beckmann E, Downing KH (1990) Model for the structure of bacteriorhodopsin based on high-resolution electron cryo-microscopy. J Mol Biol 213:899–929

Hobot JA, Villiger W, Escaig J, Maeder M, Ryter A, Kellenberger E (1985) The shape and fine structure of the nucleoid observed on sections of ultrarapid frozen and cryosubstituted bacteria. J Bacteriol 162:960–971

Humbel B, Müller M (1986) Freeze substitution and low temperature embedding. In: Müller M, Becker RP, Boyde A, Wolosewick JJ (eds) The science of biological specimen preparation 1985. AMF O'Hare, SEM Inc., pp 175–183

Jin L, Milazzo AC, Kleinfelder S, Li S, Leblanc P, Duttweiler F, Bouwer JC, Peltier ST, Ellisman MH, Xuong NH (2008) Applications of direct detection device in transmission electron microscopy. J Struct Biol 161:352–358

Kellenberger E (1991) The potential of cryofixation and freeze substitution: observations and theoretical considerations. J Microsc 163:183–203

Kelly DF, Dukovski D, Walz T (2008) Monolayer purification: a rapid method for isolating protein complexes for single-particle electron microscopy. Proc Natl Acad Sci USA 105:4703–4708

Kremer JR, Mastronarde DN, McIntosh JR (1996) Computer visualization of three-dimensional image data using IMOD. J Struct Biol 116:71–76

Lucic V, Leis A, Baumeister W (2008) Cryo-electron tomography of cells: connecting structure and function. Histochem Cell Biol 130:185–196

Marko M, Hsieh C, Schalek R, Frank J, Mannella C (2007) Focused-ion-beam thinning of frozen-hydrated biological specimens for cryo-electron microscopy. Nat Methods 4:215–217

Marsh BJ, Mastronarde DN, Buttle KF, Howell KE, McIntosh JR (2001) Organellar relationships in the Golgi region of the pancreatic beta cell line, HIT-T15, visualized by high resolution electron tomography. Proc Natl Acad Sci USA 98:2399–2406

McIntosh JR (2001) Electron microscopy of cells: a new beginning for a new century. J Cell Biol 153:25–32

McIntosh JR (2007) Cellular electron microscopy. Academic, San Diego

McIntosh JR, Grishchuk EL, Morphew MK, Efremov AK, Zhudenkov K, Volkov VA, Cheeseman IM, Desai A, Mastronarde DN, Ataullakhanov FI (2008) Fibrils connect microtubule tips with kinetochores: a mechanism to couple tubulin dynamics to chromosome motion. Cell 135:322–333

Medalia O, Weber I, Frangakis AS, Nicastro D, Gerisch G, Baumeister W (2002) Macromolecular architecture in eukaryotic cells visualized by cryoelectron tomography. Science 298:1155–1157

Mercogliano CP, DeRosier DJ (2007) Concatenated metallothionein as a clonable gold label for electron microscopy. J Struct Biol 160:70–82

Millen JI, Pierson J, Kvam E, Olsen LJ, Goldfarb DS (2008) The luminal N-terminus of yeast Nvj1 is an inner nuclear membrane anchor. Traffic 9:1653–1664

Miyazawa A, Fujiyoshi Y, Unwin N (2003) Structure and gating mechanism of the acetylcholine receptor pore. Nature 423:949–955

Müller M (1992) The integrating power of cryofixation-based electron microscopy in biology. Acta Microsc 1:37–44

Müller M, Marti T, Kriz S (1980) Improved structural preservation by freeze substitution. In: Brederoo P, de Priester W (eds) Proceedings of the 7th European congress on electron microscopy. Leiden University Press, Leiden, pp 720–721

Murata K, Mitsuoka K, Hirai T, Walz T, Agre P, Heymann JB, Engel A, Fujiyoshi Y (2000) Structural determinants of water permeation through aquaporin-1. Nature 407:599–605

Murk JL, Posthuma G, Koster AJ, Geuze HJ, Verkleij AJ, Kleijmeer MJ, Humbel BM (2003) Influence of aldehyde fixation on the morphology of endosomes and lysosomes: quantitative analysis and electron tomography. J Microsc 212:81–90

Nicastro D, Schwartz C, Pierson J, Gaudette R, Porter ME, McIntosh JR (2006) The molecular architecture of axonemes revealed by cryoelectron tomography. Science 313:944–948

Nickell S, Kofler C, Leis AP, Baumeister W (2006) A visual approach to proteomics. Nat Rev Mol Cell Biol 7:225–230

Perkins GA, Renken CW, Frey TG, Ellisman MH (2001) Membrane architecture of mitochondria in neurons of the central nervous system. J Neurosci Res 66:857–865

Perktold A, Zechmann B, Daum G, Zellnig G (2007) Organelle association visualized by three-dimensional ultrastructural imaging of the yeast cell. FEMS Yeast Res 7:629–638

Peters PJ, Pierson J (2008) Immunogold labeling of thawed cryosections. Methods Cell Biol 88:131–149

Plitzko JM, Rigort A, Leis A (2009) Correlative cryo-light microscopy and cryo-electron tomography: from cellular territories to molecular landscapes. Curr Opin Biotechnol 20:83–89

Quintana C, Lopez-Iglesias C, Laine-Delaunay MC (1991) (3-Cryo) methods (cryofixation, cryosubstitution and cryoembedding) for processing of tissues for ultrastructural and immunocytochemical studies. Application to oviduct cells of laying quail. Biol Cell 72:167–180

Salje J, Zuber B, Löwe J (2009) Electron cryomicroscopy of *E. coli* reveals filament bundles involved in plasmid DNA segregation. Science 323:509–512

Sani M, Allaoui A, Fusetti F, Oostergetel GT, Keegstra W, Boekema EJ (2007) Structural organization of the needle complex of the type III secretion apparatus of *Shigella flexneri*. Micron 38:291–301

Sartori N, Bednar J, Dubochet J (1996) Electron-beam-induced amorphization of ice III or IX obtained by high-pressure freezing. J Microsc 182:163–168

Sartori A, Gatz R, Beck F, Rigort A, Baumeister W, Plitzko JM (2007) Correlative microscopy: bridging the gap between fluorescence light microscopy and cryo-electron tomography. J Struct Biol 160:135–145

Sartori Blanc N, Studer D, Ruhl K, Dubochet J (1998) Electron beam-induced changes in vitreous sections of biological samples. J Microsc 192:194–201

Schwartz CL, Sarbash VI, Ataullakhanov FI, McIntosh JR, Nicastro D (2007) Cryo-fluorescence microscopy facilitates correlations between light and cryo-electron microscopy and reduces the rate of photobleaching. J Microsc 227:98–109

Singh G, Rice P, Mahajan RL, McIntosh JR (2009) Fabrication and characterization of a carbon nanotube-based nanoknife. Nanotechnology 20:95701

Stark H (2002) Three-dimensional electron cryomicroscopy of ribosomes. Curr Protein Pept Sci 3:79–91

Stark H, Zemlin F, Boettcher C (1996) Electron radiation damage to protein crystals of bacteriorhodopsin at different temperatures. Ultramicroscopy 63:75–79

Steinbrecht RA, Müller M (1987) Freeze-substitution and freeze-drying. Cryotechniques in biological electron microscopy. Springer, Berlin, pp 149–172

Studer D, Michel M, Wohlwend M, Hunziker EB, Buschmann MD (1995) Vitrification of articular cartilage by high-pressure freezing. J Microsc 179:321–332

Studer D, Graber W, Al-Amoudi A, Eggli P (2001) A new approach for cryofixation by high-pressure freezing. J Microsc 203:285–294

Studer D, Humberl BM, Chiquet M (2008) Electron microscopy of high pressure frozen samples: bridging the gap between cellular ultrastructure and atomic resolution. Histochem Cell Biol 130:877–889

Tomova C, Geerts WJ, Müller-Reichert T, Entzeroth R, Humbel BM (2006) New comprehension of the apicoplast of Sarcocystis by transmission electron tomography. Biol Cell 98:535–545

Tomova C, Humbel BM, Geerts WJC, Entzeroth R, Holthuis JCM, Verkleij AJ (2009) Membrane contact sites between apicoplast and ER in *Toxoplasma gondii* revealed by electron tomography. Traffic. doi:10.1111/j.1600-0854.2009.00954.x

van Heel M, Harauz G, Orlova EV, Schmidt R, Schatz M (1996) A new generation of the IMAGIC image processing system. J Struct Biol 116:17–24

van Heel M, Gowen B, Matadeen R, Orlova EV, Finn R, Pape T, Cohen D, Stark H, Schmidt R, Schatz M, Patwardhan A (2000) Single-particle electron cryo-microscopy: towards atomic resolution. Q Rev Biophys 33:307–369

van der Wel N, Hava D, Houben D, Fluitsma D, van Zon M, Pierson J, Brenner M, Peters PJ (2007) *M. tuberculosis* and *M. leprae* translocate from the phagolysosome to the cytosol in myeloid cells. Cell 129:1287–1298

Wider G, Wüthrich K (1999) NMR spectroscopy of large molecules and multimolecular assemblies in solution. Curr Opin Struct Biol 9:594–601

Yonekura K, Maki-Yonekura S, Namba K (2003) Complete atomic model of the bacterial flagellar filament by electron cryomicroscopy. Nature 424:643–650

Yu X, Jin L, Zhou ZH (2008) 3.88 A structure of cytoplasmic polyhedrosis virus by cryo-electron microscopy. Nature 453:415–419

Zeuschner D, Geerts WJ, van Donselaar E, Slot JW, Koster AJ, Klumperman J (2005) Immuno-electron tomography of ER exit sites reveals the existence of free COPII-coated transport carriers. Nat Cell Biol 8:377–383

Zhang P, Bos E, Heymann J, Gnaegi H, Kessel M, Peters PJ, Subramaniam S (2004) Direct visualization of receptor arrays in frozen-hydrated sections and plunge-frozen specimens of *E. coli* engineered to overproduce the chemotaxis receptor Tsr. J Microsc 216:76–83